



Cite this: *Phys. Chem. Chem. Phys.*,  
2024, 26, 2732

## A review of stimuli-responsive polymer-based gating membranes

Stefanie Uredat, <sup>a</sup> Aditi Gujare, <sup>†b</sup> Jonas Runge, <sup>†a</sup> Domenico Truzzolillo, <sup>b</sup> Julian Oberdisse <sup>†b</sup> and Thomas Hellweg <sup>\*a</sup>

The formation and properties of smart (stimuli-responsive) membranes are reviewed, with a special focus on temperature and pH triggering of gating to water, ions, polymers, nanoparticles, or other molecules of interest. The review is organized in two parts, starting with all-smart membranes based on intrinsically smart materials, in particular of the poly(*N*-isopropylacrylamide) family and similar polymers. The key steps of membrane fabrication are discussed, namely the deposition into thin films, functionalization of pores, and the secondary crosslinking of pre-existing microgel particles into membranes. The latter may be free-standing and do not necessitate the presence of a porous support layer. The temperature-dependent swelling properties of polymers provide a means of controlling the size of pores, and thus size-sensitive gating. Throughout the review, we highlight “positive” (gates open) or “negative” (closed) gating effects with respect to increasing temperature. In the second part, the functionalization of porous organic or inorganic membranes of various origins by either microgel particles or linear polymer brushes is discussed. In this case, the key steps are the adsorption or grafting mechanisms. Finally, whenever provided by the authors, the suitability of smart gating membranes for specific applications is highlighted.

Received 23rd October 2023,  
Accepted 23rd December 2023

DOI: 10.1039/d3cp05143a

rsc.li/pccp

### I. Introduction

In this article, recent progress in the formation, study, and application of smart membranes based on stimuli-responsive polymers is reviewed. Such membranes are designed to undergo reversible structural changes in response to external stimuli, such as temperature, pH, light, or electric fields. This is obtained by incorporating responsive materials or additives, which allow membranes to selectively swell, shrink, and thus change their permeability in the presence of specific triggers.

Typical applications are based on the controllable semi-permeability of membranes, allowing opening or closing of passages (“gating”) using external control parameters. For instance, stimuli-responsive membranes have emerged as a promising technology in wastewater remediation, offering enhanced control and efficiency in contaminant removal.<sup>1</sup> Stimuli-responsive membranes have also gained significant interest in the field of gas and other separation processes like distillation, adsorption, extraction, and crystallization due to their ability to control selectively gas transport and segregation

properties.<sup>2</sup> One of the most covered targets is the separation of carbon dioxide (CO<sub>2</sub>) from gas mixtures, especially in the context of mitigating greenhouse gas emissions and addressing climate change. Also, CO<sub>2</sub> may be used as a stimulus.<sup>3–5</sup> Yet another important application is drug delivery, with control of release induced by, *e.g.*, local heating.<sup>6</sup> As a last example, one may also make use of the change in optical properties as one approaches phase transitions, like cloud points, or of other changes in optical activity controlled by temperature.<sup>7</sup>

Stimuli-responsive polymer chains are often the basic unit providing smartness, *i.e.* their conformational changes provide control over gating by external stimuli. The gating properties of smart membranes, which may be free-standing or supported by some substrate depend on both the molecular properties of the polymer, in particular its swelling, and on the membrane geometry. The same polymer may, *e.g.*, inhibit the passage of some solute through pores in the substrate by swelling and thereby filling the pore, or allow the passage to some other solute across its swollen, less concentrated structure in an all-smart membrane. In the present review, we attempt to highlight wherever known if the system possesses a “positive” or “negative” gating effect, as illustrated in Fig. 1(a). Here “positive” means that increasing the temperature (which is the most common control parameter) opens the gates, and *vice versa*. A possible mechanism based on pore size has been discussed already 15 years ago by Alem *et al.*,<sup>8</sup> see Fig. 1(b).

<sup>a</sup> Department of Physical and Biophysical Chemistry, Bielefeld University, Universitätsstr. 25, 33615 Bielefeld, Germany. E-mail: thomas.hellweg@uni-bielefeld.de

<sup>b</sup> Laboratoire Charles Coulomb (L2C), University of Montpellier, CNRS, 34095 Montpellier, France. E-mail: julian.oberdisse@umontpellier.fr

† These authors have contributed equally to the review article.



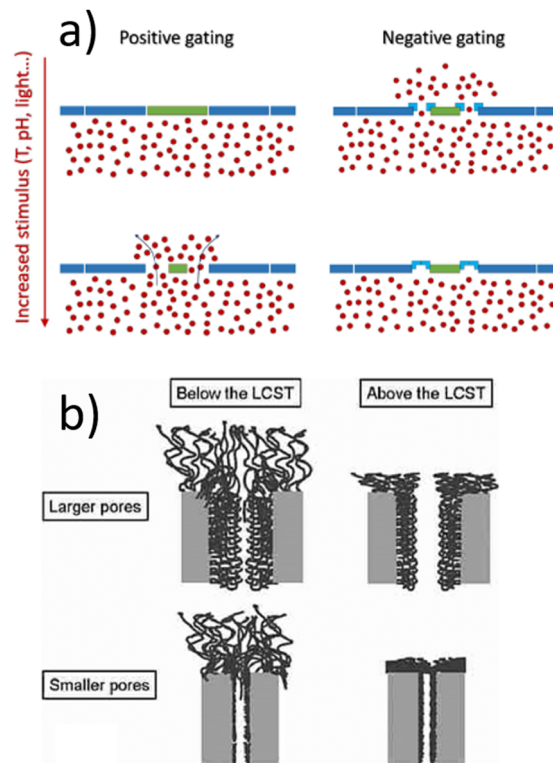


Fig. 1 (a) Illustration of positive (resp. negative) gating effect with temperature induced by T-dependent polymer swelling as discussed in this review. (b) Schematic representation of the two proposed water permeation control mechanisms depending on the size ratio of polymer layer to membrane pore diameter. Smaller pores are blocked above LCST by the collapsed polymer layer of the membrane surface whereas larger pores are opened above the LCST. B: reproduced with permission from H. Alem, A.-S. Duwez, P. Lussis, P. Lipnik, A.M. Jonas and S. Demoustier-Champagne, *J. Membr. Sci.*, 2008, **308**(1–2), 75.

Two stimuli have been extensively studied in the literature, temperature and pH. Concerning control of polymer swelling by temperature, the existence of a lower critical solution temperature (LCST), or an upper one (UCST), or possibly both, governs the solubility of the polymer in the solvent. The most investigated temperature sensitive polymer exhibiting a LCST close to body temperature ( $>33\text{ }^{\circ}\text{C}$ ) is the poly(*N*-substituted acrylamide) family (like pNIPAM), with variations extending typically between poly(*N*-*n*-propylacrylamide) ( $21\text{ }^{\circ}\text{C}$ ) and poly(*N*-isopropylmethacrylamide) ( $44\text{ }^{\circ}\text{C}$ ), depending moreover on deuteration.<sup>9,10</sup> Other related polymers are poly(*N,N'*-diethyl acrylamide) exhibiting a LCST in the range  $26\text{--}35\text{ }^{\circ}\text{C}$ .<sup>6</sup> Another, widely explored family is caprolactam, for instance poly(vinylcaprolactam) (pVCL) with a LCST in the range of  $32\text{--}34\text{ }^{\circ}\text{C}$ .<sup>11</sup> If microgels are employed, the most common primary (internal) crosslinker is *N,N'*-methylenebisacrylamide (BIS).<sup>12–15</sup> However, also other cross-linkers were already used e.g. different methacrylamides,<sup>16</sup> divinylbenzene<sup>17</sup> or cleavable cross-linkers.<sup>18</sup>

The reference polymer pNIPAM, *e.g.*, has been proposed as micro-actuator, in particular with linear swelling properties for certain microgel architectures.<sup>9</sup> that can be employed in

tunable coatings to trigger the adsorption/desorption of biological cells.<sup>19–21</sup> A similar application based on chains (as opposed to microgel particles) focusing on proteins has been proposed by Ulbricht and Yang.<sup>22</sup> Besides the monomer chemistry, the network connectivity also impacts macroscopic properties, and thus possibly gating. For instance, the control of mechanical properties by crosslinking has been highlighted in recent work by Kim *et al.*<sup>23</sup> in which the authors synthesized thin hydrogels where entanglements greatly outnumber cross-links. Such hydrogels enable transmission of tension through the network, while the sparse crosslinks prevent the polymer chains from disentangling. In this case, the large number of entanglements favors a more ductile/less brittle behavior under stress, leading to higher toughness and fatigue resistance.

We start with a short outline of general properties in Section II. Review articles with a similar scope have been published by Liu *et al.*<sup>24</sup> in 2016 and more recently by Pan *et al.*<sup>25</sup> in 2023, highlighting different types of responsiveness, and how the positive and negative gating with the different stimuli works. We propose here to review very recent contributions together with some of the older but groundbreaking articles. Section III of this review will be devoted to the discussion of “all-smart” membranes, and Section IV to “functionalized porous” membranes. Section III is further divided into two subsections where we discuss secondary crosslinking and deposition techniques. Analogously, Section IV is also divided in 2 subsections on the fabrication of porous membranes and their subsequent functionalization. In all cases, examples mostly in view of gating applications will be provided, differentiating where-ever possible “positive” from “negative” gating properties as illustrated in Fig. 1. These sections will be followed by a conclusion which also gives some outlook with respect to future research and promising new ideas.

## II. General properties and formulation of stimuli-responsive membranes

Temperature and pH are the most common external stimuli, and their effect on the conformation of polymers is to modify the degree of swelling by solvent, and thus the spatial extension of the molecules. The control of swelling by temperature is related to the transition from good to bad solvent properties, *e.g.* to the LCST of pNIPAM or poly(ethylene glycol) (PEG) as discussed in the introduction. Due to the change in volume, and to possible differences in the LCST of the single chains, the temperature where the volume shrinks has a separate name, the volume phase transition temperature (VPTT). Above the LCST/VPTT, such polymer chains or microgels prefer a relatively low hydration, which is the case in the collapsed state.<sup>26</sup> Control by pH is based on electrostatic interactions between monomers which are themselves regulated by reversible protonation/deprotonation reactions, altering the membrane's charge and permeability characteristics. These effects rely on the presence of weak acidic or basic groups, the  $\text{pK}_a$  of which is however usually slightly different from the one of the



corresponding isolated monomers due to the interaction with neighboring groups and crosslinkers. The higher the cross-linking density, the lower the permeability, especially for high molecular weight solutes. Typical examples of pH-sensitive polymers with anionic groups that can be used to form pH sensitive membranes are poly(carboxylic acids) as poly(acrylic acid) or poly(methacrylic acid), or polysulfonamides (derivatives of *p*-aminobenzenesulfonamide), while other pH sensitive polymers contain sulfonamide groups.<sup>27</sup> Examples of cationic polyelectrolytes are poly(*N,N*-diakyl aminoethyl methacrylates),<sup>28</sup> poly(lysine),<sup>29</sup> poly(ethylenimine) (PEI),<sup>30</sup> and chitosan.<sup>31</sup> By tuning the pH of the feed gas or the membrane itself, the transport of, *e.g.*, CO<sub>2</sub> can be selectively enhanced while minimizing the permeation of other gases.<sup>2</sup>

The synthesis of stimuli-responsive polymer chains themselves is outside the scope of the present review. The reader is probably aware that usually either controlled radical (or living) polymerization, or free radical precipitation-polymerization is described in the literature.<sup>32–38</sup> In the following two sections, two different approaches to the formation of smart polymer-based gating membranes are discussed. First, in Section III, the formation of an “all smart” membrane is targeted, either as a polymer macrogel, or as polymer gel obtained from previously synthesized microgel particles. As already mentioned in the introduction, the crosslinked state of the polymer chains is of primary importance, in particular for “all smart” membranes. Crosslinked membranes are obtained by covalently binding individual chains and make volume spanning networks *via* crosslinking coupling reactions.<sup>39</sup> The latter normally lead to random network structures, as they have been studied by scattering techniques applied to macrogels.<sup>40,41</sup> These structures cannot fully self-optimize themselves due to permanent and rigid primary crosslinking to absorb or release very high content of solvent. On the other hand, the additional external crosslinking of already internally crosslinked microgel particles offers the possibility to optimize features like mechanical strength and swelling. We call “secondary crosslinking” this additional chemical crosslinking step in the case of microgel particles which are already internally crosslinked, often using BIS. Several of these protocols, *e.g.* based on photocrosslinking,<sup>18,42</sup> or with chemical crosslinking using glutaraldehyde in presence of primary amines on the chain,<sup>43,44</sup> will be also reviewed. The requirement on the secondary crosslinker is that it is incorporated in the primary polymer network without inducing any crosslinking, while this is triggered later in the membrane preparation process.

Secondly, in Section IV, we discuss the functionalization of porous non-stimuli responsive membranes by stimuli-responsive polymer as proposed in the literature. This functionalization relies on a grafting or adsorption step, and usually leads to the formation of a stimuli-responsive brush. The supporting membranes of smart coatings are often non-crosslinked glassy polymers<sup>45,46</sup> or carbon nanotube grids,<sup>47</sup> with high mechanical strength. These porous support membranes can also be woven tissues, or non-woven substrates made of fibers obtained *e.g.* by electrospinning. Non-woven

porous functionalized membranes are known to be abrasion and heat resistant, and show high flexibility and elasticity.<sup>48</sup> Moreover, they have been proposed for applications in filtration<sup>49</sup> and enzyme immobilization.<sup>50</sup> The membrane optimization in response to the external stimulus may be complicated by both the difficulty in obtaining a homogenous coating on the sub-nanometric scale, and the typical lack of responsiveness of the glassy polymer scaffold of the membrane.

### III. All-smart membranes

All-smart membranes can be produced either from stimuli-responsive polymer chains or microgel particles. The formation of membranes from primary microgel particles may be quite efficient due to pre-ordering of the particles in a regular arrangement. Whatever the starting material, the fundamental process can be divided into a deposition step, where a thin, usually sub-micron layer is formed on a substrate. In a second step, the polymer chains (or microgels) are crosslinked, and finally the membrane is removed from the substrate, providing a floating and possibly free-standing membrane. In some cases, discussed below, the secondary crosslinking has not been attempted yet, or the stimuli-responsiveness is still missing. We nonetheless kept such results of the literature as illustrative steps paving the way to the final goal.

Several secondary crosslinking techniques exist, either based on electron or UV irradiation, or on chemical reactions, for instance of glutaraldehyde with amines. We introduce the different crosslinking methods first in Section III.1, before discussing the deposition protocols and the resulting membranes below. For the deposition step, any physical (adhesion for dip-coating, centrifugation for spin-coating) or physico-chemical force (*i.e.*, self-assembly or interfacial techniques based on selective solvents or incompatible moieties) may be used. Examples of membranes obtained by different deposition protocols are discussed in Section III.2.

#### III.1 Secondary crosslinking

Irradiation by an electron-beam is a well-known technique which has been used, *e.g.*, in graft polymerization of acrylamide on linear low-density polyethylene film.<sup>51</sup> Radiation-induced grafting on a substrate to introduce hydrophilicity has applications in membrane filtration.<sup>51</sup> Although the so-formed membranes are typically not switchable, this technique has been exploited for secondary cross-linking of microgel thin films with tunable properties. For example, microgel films were obtained by precipitation polymerization of aromatic comonomer N-benzylhydrylacrylamide (BHAm) with NIPAM using BIS as a primary crosslinker. The deposition of these poly(NIPAM-*co*-BHAm) microgels was done on gold coated Si-wafers which were subsequently irradiated with an electron flood gun. The free standing nanomembrane made of microgels was obtained by dissolution of the gold layer. Such freestanding thermo-responsive membranes could be transferred to the chosen substrate, thereby increasing the number of possible applications



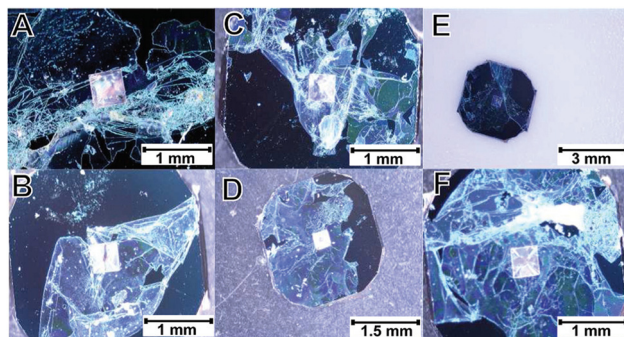


Fig. 2 Photograph of microgel membranes which were secondarily crosslinked by an electron beam on a silicon chip. The white square is a funnel hole with a silicon nitride membrane for resistance measurements. Reprinted with permission from J. Bookhold, M. Dirksen, L. Wiedemeier, S. Knust, D. Anselmetti, F. Paneff, X. Zhang, A. Götzhäuser, T. Kottke and T. Hellweg, *Soft Matter*, 2021, **17**(8), 2205.

(see Fig. 2).<sup>52</sup> The resulting membranes show thermo-responsive behavior, by shrinking above their VPTT and swelling below it, and show regulation of ion flow, with a negative gating effect, *i.e.* increased resistance in the collapsed high-T state.

UV crosslinking is considerably easier to use, and less radiation damage is produced. Typical UV-sensitive monomers are benzophenone and its derivatives.<sup>53</sup> Such photoinitiators (PIs) can be classified into type I and type II PIs.<sup>54</sup> Type I PIs dissociate after irradiation forming two radicals. Type II PIs need a co-initiator because they undergo photoreduction.

When photosensitive monomers such as 2-hydroxy-4-(methacryloyloxy)-benzophenone (HMABP) are added into a microgel polymer system, the secondary crosslinking can be obtained with UV light irradiation. Dirksen *et al.*<sup>18,42</sup> synthesized BIS-crosslinked poly(NIPAM-*co*-HMABP) microgels and spin coated a silicon wafer with the microgel. Freestanding membranes made of 2–3 layers of the original microgels were achieved after irradiation of the sample with UV light. They performed temperature-dependent resistance measurements and could show a switch in resistance at the VPTT of the microgel.

As one can see in Fig. 3(a), the resistivity increases abruptly with temperature, and the system displays thus a negative gating effect. If a degradable crosslinker such as 2,2'-(bisacrylamino)diethyl disulfide (BAC) is used instead of BIS, the gating behaviour can be inverted if the cross-linker is cleaved with a solution of 1,4-dithiothreitol (1 mM) after membrane formation (Fig. 3(b)) by maintaining the stability of the membranes.<sup>18</sup> This allows switching from a negative to a positive gating effect.

The contribution by Sabadasch *et al.*<sup>55</sup> shows that the UV cross-linked smart membranes can be loaded with nanoparticles (here palladium) that can be used in catalytic applications. The free-standing photo-crosslinked membranes were deposited on a nylon mesh to achieve higher mechanical stability (see Fig. 4). Such supported nanoparticle – membrane hybrids allow easy separation from the reaction medium and recycling of the catalyst. Such membranes might also be useful in microfluidic lab-on-a-chip applications. However, this still remains to be explored. Also, the thermo-response of the

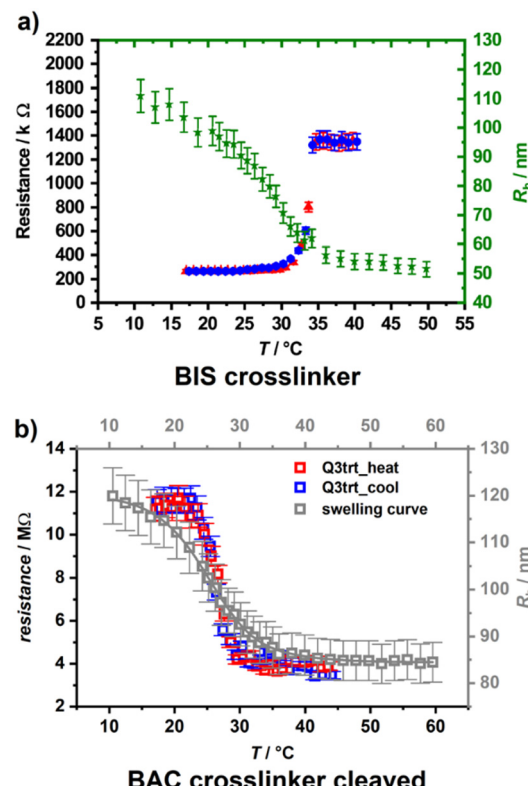


Fig. 3 Resistance as a function of temperature for a p(NIPAM-*co*-HMABP) membrane with 5 mol% HMABP comonomer feed and 5 mol% crosslinker. The measuring cycle consists of a heating curve (red) and a cooling curve (blue), compared to the swelling curve (green/grey) of the corresponding microgel. (a) An abrupt increase of resistance is observed above the VPTT of pNIPAM, evidencing a negative gating effect for BIS crosslinked microgel membranes. Reproduced with permission from M. Dirksen, T. Brändel, S. Großkopf, S. Knust, J. Bookhold, D. Anselmetti and T. Hellweg, *RSC Adv.*, 2021, **11**(36), 22014. (b) Inverted gating observed when replacing BIS by the degradable crosslinker BAC. Reprinted with permission from Dirksen, M., Fandrich, P., Goett-Zink, L., Cremer, J., Anselmetti, D., & Hellweg, T. Langmuir. Copyright 2022 American Chemical Society.

membranes was not yet exploited to achieve better control of the reaction.

The crosslinking mechanism of primary amines introduced by copolymerization with glutaraldehyde is different from most other crosslinking reagents. In particular, it is not based on the simple mechanism of Schiff base linkages on both ends of the glutaraldehyde. In parallel with the crosslinking reaction, the polymerization of glutaraldehyde *via* aldol condensation may take place, enabling the formation of links between particles.<sup>56</sup>

Swelling properties of membranes capable of gating may also be generated with non-synthetic polymers. For example, Tokarev *et al.*<sup>57</sup> prepared a highly porous alginate membrane. A thin film of sodium alginate and diamine-PEG film was spin-coated on a wafer. Scanning probe microscopy measurements confirmed a phase separation of the two monomers. By addition of calcium ions, ionic crosslinking of alginate was induced. Afterwards, the membrane was formed by rinsing with water to elute the diamine-PEG. The membrane thickness was

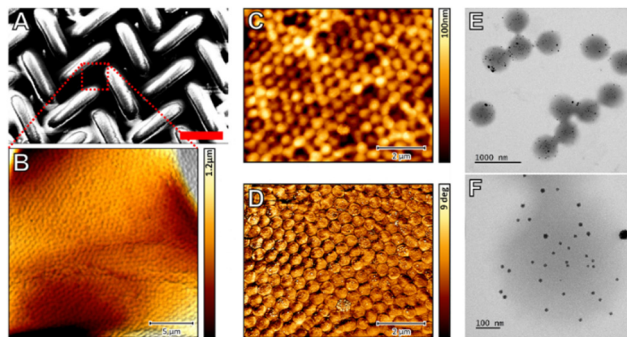


Fig. 4 The free-standing microgel membrane was transferred after UV-crosslinking to a nylon support mesh to achieve better mechanical stability. (A) SEM image, (B) AFM height image. (C) A high resolution image of the crosslinked microgel membrane on the support mesh is shown. (D) In the corresponding AFM phase image incorporated palladium nanoparticles are visible. In (E) and (F) TEM images of the microgels prior to the secondary crosslinking are shown. The incorporated palladium nanoparticles are clearly visible. (A)–(D): Reprinted with permission from V. Sabadasch, M. Dirksen, P. Fandrich, J. Cremer, N. Biere, D. Anselmetti and T. Hellweg, *ACS Appl. Mater. Interfaces*, 2022, **14**(43), 49181. Copyright 2023 American Chemical Society. (E) and (F): Reproduced with permission from V. Sabadasch, M. Dirksen, P. Fandrich and T. Hellweg, *Front. Chem.*, 2022, **10**, 889521.

controlled by the concentration of the casting solution. The membrane was stable below pH 8 and showed pH-dependent swelling in the range going from pH 2 up to pH 6. Similar to thermo-responsive membranes a sharp swelling transition was observed between pH 4 and 5 with an inflection point of 4.6. The inflection point was in the range of the reported  $pK_a$  of alginate. The pores of the membrane were found to be fully closed at pH values of 4.6 and higher.

### III.2 Deposition protocols and resulting membranes

Having the different secondary crosslinking techniques at hand, we can now turn to the discussion of membrane formation, from polymer deposition to applications. Solvent casting is the most ancient technique. Polymer and solvent are the main components of an initial solution, but various additives can also be adjoined. As an example, Peng *et al.*<sup>58</sup> investigated the pervaporation properties of PDMS-based membranes filled with carbon molecular sieve for benzene removal from aqueous media. The membrane was formed from a paste of 107 RTV silicone rubber, a solvent, a catalyst, and a cross-linking agent, which was cast with a doctor blade, dried and cured. These membranes showed an important increase of the permeation for increasing operating temperature, *i.e.* negative gating.

Still *et al.*<sup>44</sup> used the evaporating drop method which is drying the mixture of microgel with the secondary crosslinker (*e.g.* glutaraldehyde) and dry on a substrate to fabricate a freestanding temperature-sensitive membrane made of p(NIPAM-*co*-AEMA), where the comonomer is 2-aminoethyl methacrylate. Fig. 5 shows the so obtained freestanding membrane on the right. At higher temperatures the membrane shrinks and becomes darker due to its higher density: the light transmittance can thus be controlled, with a negative gating effect.

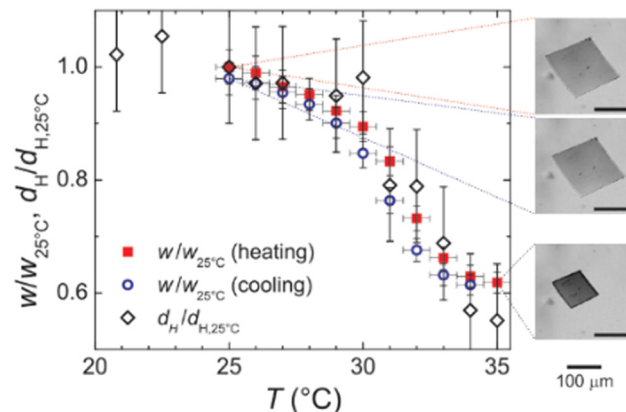


Fig. 5 Evolution of sample size with temperature of square-cut hydrogel films in water during heating (solid red squares) and cooling (open blue circles). The width  $w$  is renormalized to the one at 25 °C. The normalized hydrodynamic diameter  $d_H/d_H$ , 25 °C of the constituent particles is shown (open diamonds) in the same diagram ( $d_H = 1.53 \mu\text{m}$  at 25 °C). Pictures on the right show micrographs of the film at 25 °C (before and after heating cycle) and 35 °C, respectively. Reproduced with permission from Still *et al.* (2015), Temperature-Sensitive Hydrogel-Particle Films from Evaporating Drops, *Adv. Mater. Interfaces*, **2**(16). ©2015 WILEY-VCH Verlag GmbH & Co. KGaA, Weinheim.

On the left, the reversible change in size with temperature is shown.

Self-assembly in bulk or at interfaces is an elegant way to form thin, nanostructured polymer membranes. Several techniques relying on the physico-chemical preference of certain molecules (or moieties, in particular blocks of block copolymers) for solvents have been used in the past, in most cases however not for smart membranes. Molecular monolayers, *e.g.*, may be spread at the air–water or oil–water interface. Ahmed *et al.*<sup>59</sup> employed amphiphilic diblock copolymers that have been cross-linked in both monolayer at the air–water interface and bilayer assemblies. Similarly, El-Haitami *et al.*<sup>60</sup> proposed a method to obtain ultrathin membranes with good mechanical properties by *in situ* synthesis at the air–water interface of a 2D semi-interpenetrating polymer network. Very recently, Coppola *et al.*<sup>61</sup> fabricated *in situ* a polymer membrane, simply by injecting drops of polymer solutions at the oil–water interface.

Self-assembly as mechanism of nanostructure formation is based on the preference of certain blocks of a block copolymer to regroup in the bulk, and thus form organized supramolecular structures. Cetintas *et al.*<sup>62</sup> present fully reversible thermo-responsive nanoporous membranes fabricated by self-assembly and non-solvent induced phase separation (NIPS) of polystyrene-poly(*N*-isopropylacrylamide) (PS-*b*-pNIPAM) block copolymers. The sudden replacement of a good solvent of both blocks by a selective solvent, *i.e.* non-solvent for one of the blocks, triggers a microphase separation leading to a porous system after drying. A variety of PS-*b*-pNIPAM block copolymers were synthesized by reversible addition-fragmentation chain transfer (RAFT) polymerization and the reaction conditions were optimized. The target copolymers



featured: (1) a thermo-responsive pNIPAM block, (2) a majority PS fraction, and (3) a well-defined high molecular weight, which are requirements for successful fabrication of free-standing responsive membranes using NIPS. The resulting membranes exhibited a worm-like cylindrical morphology with interconnected nanopores. These membranes exhibit a positive gating effect, as the permeability for water increases with temperature, and is reversible. Polymer phase separation and self-assembly have been exploited also very recently by Willott and co-workers<sup>63</sup> to obtain pH-sensitive symmetric porous microfiltration membranes and asymmetric dense nanofiltration membranes, where the degree of responsive behavior could be tuned by the degree of cross-linking.

A more conventional method for obtaining thin layers of microgels is spin coating.<sup>64–66</sup> This technique has been extensively used to produce membranes without stimuli-responsiveness. For instance, Kang *et al.*<sup>67</sup> describe the fabrication and characterization of large-scale (> 2 cm in diameter) free-standing ultrathin PDMS membranes. Thangawng *et al.*<sup>68</sup> report a method for making ultra-thin PDMS membranes as thin as 70 nm. On the other hand, Cors *et al.* have produced stimuli-responsive microgel monolayers by spin-coating which proved to have a thermal response equivalent to the one of the individual primary microgel particles in suspension.<sup>9</sup> Such layers, however, had not yet undergone secondary crosslinking, and could be redissolved in water.

Thermo-sensitive triblock copolymers have also been deposited by spin-coating, taking advantage of their spontaneous self-assembly in bulk. Nykanen *et al.*<sup>69</sup> describe the synthesis of temperature-responsive polystyrene-*block*-poly(*N*-isopropyl-acrylamide)-*block*-polystyrene triblock copolymers, PS-*b*-pNIPAM-*b*-PS, their self-assembly and phase behavior in bulk. Moreover, they have demonstrated the formation of thermo-responsive membranes from these block copolymers. Composite membranes for separation studies were prepared by spin-coating thin films of this triblock copolymer on top of meso/macroporous polyacrylonitrile support sheet. The permeability was measured as a function of temperature using aqueous mixture of PEG with several well-defined molecular weights. The permeability showed a temperature switchable on/off behavior, where higher permeability is obtained below the transition temperature of pNIPAM, *i.e.* the system presents a negative gating effect. The molecular cutoff limits for the PEG molecules are surprisingly low, between 108 and 660 g mol<sup>-1</sup>.

Other block copolymer systems can also be used. Tang *et al.*, *e.g.*, used a selective solvent to form nanopores with a diameter of 5 nm in spin-coated symmetric triblock copolymer layers based on methacrylates and polystyrene.<sup>70</sup> The authors produced a poly(ethylene glycol methyl ether methacrylate)-*b*-PS-*b*-poly(ethylene glycol methyl ether methacrylate) (PMENMA-*b*-PS-*b*-PMENMA) mesoporous size-selective layer attached to a polyvinylidene fluoride macroporous supporting layer. The PMENMA covers the pores and its LCST in water can be tuned by the number of ethylene glycol units. Water permeability experiments showed that a higher flux of water passes through the membranes at temperatures above the LCST, suggesting

that the pore sizes are temperature controllable and that the gating effect is positive. The T-dependent size selectivity of the membranes was also investigated and a strong size-discrimination in particle permeation was found, however based on a gradual temperature response.

Finally, microgels made of NIPAM and acrylic acid have been deposited by spin-coating on silicon wafers coated with three layers, first *n*-octyltrichlorosilane and then poly(octadecene-*alt*-maleic anhydride), and with a cationic PEI layer on the surface. These thermo-responsive films show homogeneous and dense deposition in the swollen state. They also show the same behavior in their collapsed state but only at higher pH, as smaller size promotes higher packing efficiency and pH 7 or 10 makes the particles charged and results in efficient binding to the cationic PEI surface.<sup>71</sup> Monolayer deposition of such films has been obtained by S. Schmidt *et al.*<sup>64</sup> where poly(NIPAM-*co*-acrylic acid) microgel films were deposited on the PEI layer on silicon wafers. A stable monolayer was obtained at lower pH (pH = 2), while above pH 5, most of the material is desorbed because of the enhanced repulsion between the like-charged particles. Also thermo-responsive poly(NIPAM-*co*-styrene) microgel films with styrene as a comonomer to introduce amphiphilicity were deposited on glass cover slip by the same technique, spin coating, for application in cell growth and detachment.<sup>72</sup>

## IV. Functionalized porous support membranes

The production and characterization of membranes is a rather mature science, and it is not the objective of the present article to review this very broad field in detail. The formation of smart membranes may, however, be based on porous membranes without response to external stimuli, and the responsive part may be added in a second step. In Section IV.1, we review some of the more common protocols to produce porous membranes, and then discuss smart functionalization and possible applications in Section IV.2.

### IV.1 A quick overview of the fabrication of porous support membranes

A possible approach for developing polymeric membranes is electrospinning forming non-woven tissues. Thereby, polymeric membranes have been prepared for applications in filtration and biological applications such as enzyme immobilization. After functionalization, such membranes are abrasion- and temperature- resistant, showing a high flexibility and elasticity.<sup>48</sup> Sometimes hollow fibers are also used.<sup>73</sup> Electrospinning can be employed to fabricate non-woven hydrogels, which can be crosslinked with UV-light as done by Xu *et al.*<sup>74</sup> These authors synthesized a polymer made of NIPAM and the photo-crosslinker 4-acryloylbenzophenone (ABP). After electrospinning they crosslinked the nonwoven polymer into a temperature sensitive membrane.



Carbon nanotubes have also been proposed as support for smart functionalization, taking advantage of their exceptional mechanical properties.<sup>75</sup> Due to the rather small diameter and the high aspect ratio, carbon nanotubes offer a high surface area for smart functionalization, typically by “grafting-onto” reactions of preformed polymer chains, while “grafting from” is also possible.

Inducing phase separations in polymer solutions is a common way of producing pores. Porous polysulfone membranes were prepared *via* non-solvent induced phase separation (see Section III.2) with an anionic flocculant based on acrylamide and sodium acrylate (PASA), varying the PASA concentration and the temperature of the coagulation bath.<sup>76</sup> With increasing PASA concentration an increase of viscosity was observed. This lowered the solvent-non-solvent exchange rate resulting in formation of a sponge-like membrane without macrovoids at 60 °C. Membrane permeability and fouling parameters were then studied showing impact of the PASA content. The authors attribute the improvement of the antifouling performance to the higher hydrophilization of the surface of the skin layer and a higher absolute zeta potential compared to the membrane without PASA, preventing the adsorption of foulants.

Inorganic support membranes can be obtained by various techniques. Spray-coating, *e.g.*, has also been used to fabricate microporous membranes, however usually on supports, and as far as we are aware, not containing stimuli-responsive parts. A novel fabrication method based on spray coating was developed to produce a membrane supported on self-made macro-porous silicon carbide (SiC) supports for gas purification.<sup>77</sup> In another contribution, micro-filtration membranes were prepared on macro-porous plate alumina supports.<sup>78</sup> Ceramic suspension was obtained by dispersing  $\alpha$ -Al<sub>2</sub>O<sub>3</sub> powder in an aqueous solution containing polyvinyl alcohol (PVA), polyvinyl pyrrolidone (PVP), polyacrylic acid and glycerol. Then the effects of annealing conditions on the membrane morphology, pore size distribution, as well as the permeation and binding strength were investigated.

If one is interested in having pores not only of controlled size, but also with a given orientation, then anode aluminum oxide membranes (AAO) membranes are the material of choice. Feng *et al.* showed that AAO pores can be functionalized to make the membrane responsive.<sup>79</sup> Similarly, organic substrates with oriented channels have also been used,<sup>80</sup> or track-etched gold-covered arrays of parallel capillaries which have been subsequently functionalized by Lokuge *et al.*<sup>81</sup>

#### IV.2 Smart functionalization of porous support membranes and their applications

The functionalization of porous membranes with stimuli-responsive polymers has been performed following two pathways. The first one consists in fixing smart microgel particles on the surface of the membranes, and in particular in the pores, and crosslink them mutually. The advantage is that a smart particle of well-defined size, for instance with respect to the pore size, is added to the system. The second pathway is to either fix pre-existing stimuli-responsive polymer chains

(grafting onto) on the membrane, or to make them grow from the surface (grafting from) by fixing the initiator to the surface and polymerizing from there.<sup>8,82,83</sup> Applications and the special case of inorganic support membranes are also discussed.

#### Membrane functionalization by microgels

The Stamm group has a considerable record in the functionalization of microfluidic channels.<sup>84</sup> This has been continued by some former collaborators of the same group which have made further progress with functionalization by pre-formed microgel particles, and paved the way towards applications in water purification based on immobilized nanoparticles as active ingredient, or membrane anti-biofouling properties.<sup>85</sup> Maity *et al.* synthesized core-shell microgels by grafting short PEI chains onto a poly(NIPAM-*co*-glycidyl methacrylate) microgel.<sup>86</sup> In this work the major aim was to use these particles as carriers for silver nanoparticles. After loading the microgels with silver nanoparticles (or other functionalities) the microgels were suction deposited on a polyethylene terephthalate (PET) track-etched membrane. The PEI coating of the core-shell microgels allows subsequent cross-linking using glutaraldehyde. Finally, the pore size was found to increase with T, thus providing a positive gating effect. This approach was already previously proposed by the same group for making slightly different microgel-based membranes.<sup>85</sup> They also used zwitterionic microgels to optimize anti-biofouling properties of smart membranes.<sup>87</sup> Similarly, a one-step precipitation polymerization approach was used by taking 10 and 20 wt% of the vinylimidazole propane sultone with NIPAM and AEMA, with the cross-linker BIS to produce different microgels.<sup>88</sup> The microgels were again deposited by suction on a PET membrane and cross-linked by glutaraldehyde. The membranes exhibit strong anti-fouling activity and can be used to cover surfaces of different shape. The positive gating effect resulted in increased water flux. The overarching aim of these three contributions was the development of smart membranes for water purification. The group has shown that purification can be achieved by simple gating or by active components in the membranes which are metal nanoparticles or enzymes.<sup>89,90</sup>

Wessling and co-workers<sup>73</sup> developed further the approach initiated by Stamm.<sup>84</sup> Thermo-responsive PVCL microgels were immobilized on an inorganic membrane made of silicon carbide and carbon. The microgels are adsorbed on the surface by electrostatic attraction and hydrophobic interactions. Applying voltage to this conducting membrane increases the temperature and permeability, the system thus displays a positive gating effect. These membranes also show reversibility and a stable on-off switch. In Fig. 6 the temperature dependent dead-end permeation is shown for 3 consecutive heating and cooling cycles. A power of 30 W m<sup>-1</sup> was applied to heat the membrane above the VPTT. The response of permeation to temperature changes is very direct due to the fast reaction of microgels to temperature changes.<sup>91</sup>

Hollow-fiber membranes made of poly(ethersulfone) (PES) have also been modified by adsorbing microgels to make them thermoresponsive micro- and ultrafiltration membranes.



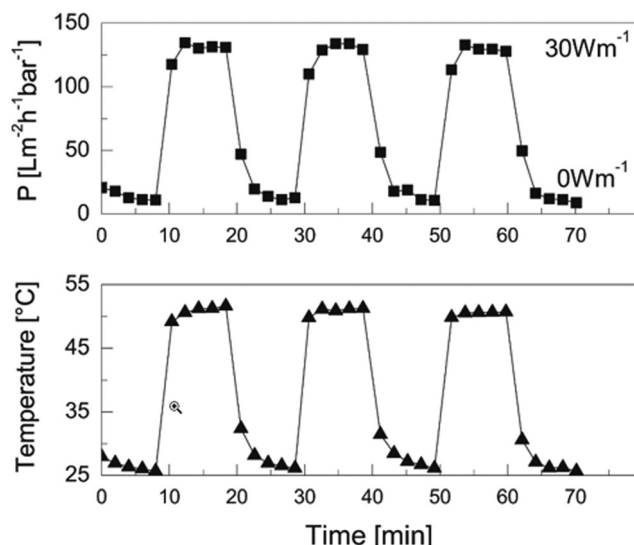


Fig. 6 The dead-end permeability ( $P$ ) through a Si-C membrane with PVCL microgel coating was measured with heating cycles of 10 min with  $30 \text{ W m}^{-1}$  of applied power. The permeability is increased due to the collapse of the microgel. Reproduced with permission from T. Lohaus, P. de Wit, M. Kather, D. Menne, N.E. Benes, A. Pich and M. Wessling, *J. Membr. Sci.*, 2017, **539**, 451.

These PES membranes were coated with PVCL-based microgels by dynamic adsorption process. The microgels conserve their thermoresponsive behavior after adsorption on the PES membrane therefore showing complete reversibility with change in temperature.<sup>92</sup> As a result, the complete retention of humic acid was obtained at low  $T$ , whereas the membrane became permeable at high  $T$ , evidencing a positive gating effect. Immobilisation of charged pNIPAM-co-acrylic acid microgel, on hollow-fiber PES membrane has also been studied. The acrylic acid comonomer was used to incorporate charge on the microgels, the main focus being on their behavior with the porous PES membrane.<sup>93</sup>

Bell *et al.*<sup>43</sup> used the pore-covering method to obtain a temperature sensitive membrane. They first synthesized microgels with a hard core and a fuzzy shell. The core was wider than the pores of the porous substrate made of PES. The microgel deposition was performed by a constant flow of dilute microgel suspension in a specially-designed 3D-printed dead-end module with a filter membrane area of  $4 \text{ cm}^2$ , producing SX-membranes (single crosslinked). In a second experiment they chemically crosslinked the so obtained microgel layers with flowing ammonium persulfate and *N,N,N',N'*-tetra-methyl-ethylenediamine-solution through the membrane, achieving a secondary or double crosslinking (DX). These authors then carried out temperature-dependent resistance measurements and provided evidence for a difference between the SX- and DX-membrane. For example, the DX-membrane showed no compression effect in contrast to the SX-membrane. The compression was used to create more densely packed multilayers, which could be fixed in this state with chemical crosslinking. The SX-membranes desorbed from the membrane surface, when

there was no more pressure/flux applied, while the DX-membrane remained intact on the surface. The higher temperature induced higher resistivity, *i.e.* this system possessed a negative gating effect.

### Membrane functionalization by polymer grafting

Grafting of polymers from the surfaces of the pores instead of depositing pre-synthesized microgel particles maybe advantageous in terms of pore coverage also deep inside the membrane. Monomers being much smaller than the microgel particles, one can imagine that they diffuse into the porous material and participate in growing polymer chains on all available surfaces. The gating response might thus be considerably sharper.

Friebe and Ulbricht<sup>83</sup> reported grafted pNIPAM *via* Atom Transfer Radical Polymerization (ATRP) in the pores of a track-etched PET membrane. They observed a significant reduction in the water permeability of the grafted membranes compared to untreated ones. Further, a thermo-responsive gating is achieved due to the thermo-responsive behavior of pNIPAM. The water permeation is strongly reduced below the LCST of pNIPAM because the polymer brush is swollen and blocks the membrane pores. ATRP grafting allows controlled functionalization in terms of layer thickness, thereby controlling the pore diameter and thus the gating effect in a more efficient manner as illustrated in Fig. 7. Functionalization of the porous materials in such a controlled manner could be further used for development in drug release and microfluidic applications.

In an already mentioned article which nicely illustrates the possible mechanisms of gating, Alem *et al.*<sup>8</sup> grafted pNIPAM *via* ATRP on a track-etched PET membrane. They analyzed the gating functionality of the membranes with conductivity measurements. For membranes with an initial pore diameter of 330 nm the conductivity increased above the LCST of NIPAM: The polymer brush collapsed and the membrane pore was not blocked anymore: a positive gating effect was observed. For membranes with an initial pore diameter of 80 nm the conductivity decreased above the LCST of NIPAM, and a negative gating effect was found. These authors proposed two different types of water permeation control mechanisms depending on the initial pore diameter (see Fig. 1): for small pores the pNIPAM layer on the membrane surface is thicker compared

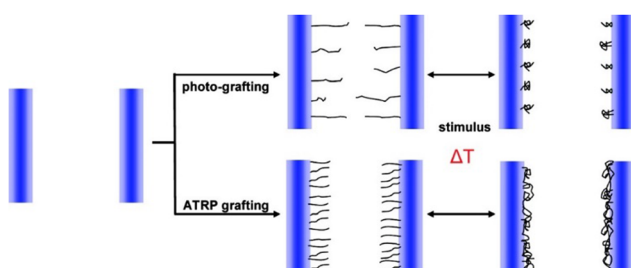
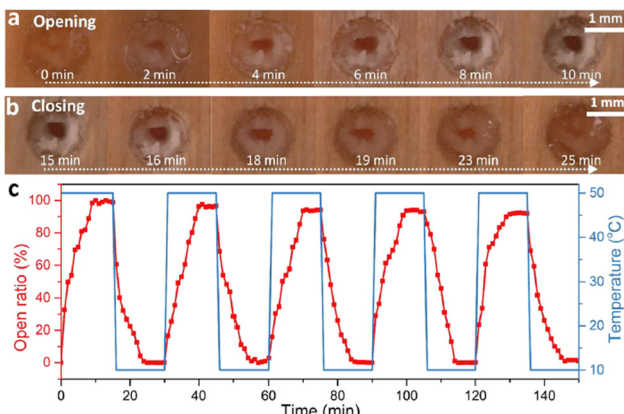


Fig. 7 Controlling the pore diameter in the submicrometer dimension by ATRP grafting for functionalization of porous thermos-responsive materials. Reprinted with permission from A. Friebe and M. Ulbricht, *Langmuir*, 2007, **23**(20), 10316. Copyright 2023 American Chemical Society.



**Fig. 8** Thermo-responsive pore behavior of smart gating wood membranes. (a) Light microscopy images of hydrogel-filled pore opening over time during heating. (b) Light microscopy images of hydrogel-filled pore closing over time during cooling. (c) Opening ratio of a hydrogel-filled pore during five heating/cooling cycles. Reprinted from Y. Ding, G. Panzarasa, S. Stucki, I. Burgert, and T. Keplinger, *ACS Sustainable Chem. Eng.* 2022, **10**, 17, 5517–5525. Copyright©2022 The Authors (CC BY-NC-ND 4.0). Published by American Chemical Society.

to the pore diameter and the pNIPAM layer inside the pores. Thus, above the LCST the polymer collapses and is forming a hydrophobic “cork” blocking the membrane pores.

Finally, it is worth mentioning the recent work by Ding *et al.*, which represents a macroscopic and thus visual illustration of gating with temperature.<sup>94</sup> The authors reported the fabrication of wood-based smart gating membranes exhibiting reversible and stable pore opening/closing under heating/cooling stimuli. The fabrication included pretreatment of a polar wood scaffold with methacrylic anhydride, followed by *in situ* polymerization of pNIPAM to fill the pores with thermoresponsive hydrogels. The thermoresponsive smart gating wood membrane pores close below LCST and open above LCST of pNIPAM (Fig. 8(a)–(c)), showing therefore positive gating.

### Some applications

Da Silva *et al.* have explored applications in catalysis of pNIPAM-functionalized PET membranes with a well-defined pore structure (200 nm channels). They used these membranes to cover a catalytically active inorganic layer containing palladium.<sup>80</sup> It was shown that the catalytic turnover could be controlled by changing temperature. At low temperatures, where the polymer is swollen, the turnover indicates that the performance of the catalyst goes up. Moreover, the authors presented a model of the CO transport and chemisorption on the polymer membrane catalyst assembly. This model points to the fact that the delay in CO chemisorption is caused by the strong affinity of the CO to the thermosensitive polymer. In addition, the authors showed that the regulation behavior of the pNIPAM modified membrane can be reversed by reducing the ratio of polymer inside the pores and the surface. This leads to an inverted behavior with respect to temperature. This inverted behavior nicely corresponds to the findings by Dirksen *et al.* for freestanding microgel membranes with catalytic activity.<sup>18</sup>

Stimuli-responsive polymers can be modified by functionalization inducing changes in membrane wetting behavior. Wetting is a property of a surface which reflects the equilibrium between the interfacial forces acting along the boundary line separating the surface, the liquid deposited on it, and the surrounding fluid. This equilibrium can be tuned by modifying the hydrophobicity of a polymer anchored on the surface. The article by Zhang *et al.* describes the fabrication of pNIPAM functionalized carbon nanotube-based smart membranes.<sup>75</sup> Nanofiber composite membranes with switchable superwettability are obtained by carbon nanotubes (CNTs) adsorption onto electrospun polyurethane (PU) nanofibers (non-woven). This structure is subsequently functionalized with pNIPAM. The authors show that pNIPAM enhances the interfacial interaction between CNTs and PU nanofibers without sacrificing the flexibility of the membrane. As a result, the membrane can be either oil- or water-permeable, at high and low temperatures, respectively. Depending on the substance to be blocked or not, the system thus represents a positive gating effect (for oil), and a negative one (for water).

An important application of membranes is therefore (ultra)-filtration. The permeation of solvent and solutes depends crucially on the physico-chemical state of the internal membrane surface. Controlling adsorption or desorption of, *e.g.*, proteins, is fundamental to designing efficient filtering membranes. Ulbricht and Yang<sup>22</sup> used benzophenone as photoinitiator to crosslink different systems of acrylamide, acrylic acid and BIS with UV light, which are adsorbed/entrapped on a porous polypropylene substrate coated with benzophenone as photoinitiator. They obtained polymer brushes on the substrate which they used to bind more lysine reversibly to the substrate surface in comparison to the unmodified membrane.<sup>22</sup>

### Inorganic substrates

Several groups have worked with smart functionalization of inorganic substrates. The latter may possess a well-defined and oriented network of pores generated by anisotropic pore growth. Feng *et al.* show that anode aluminum oxide membranes can be functionalized to make such membranes responsive.<sup>79</sup> Here, the inner surface of the pores inside the AAO are functionalized to generate polyelectrolyte-filled pH-responsive membranes. These membranes allow to regulate ion flow by changing the pH value. The authors have functionalized AAO membranes with a variety of pore sizes (25, 75 and 100 nm) by a “grafting-to” approach using poly(methacrylic acid). At pH values above the  $pK_a$  the pores in the inorganic membrane are blocked. At  $pH < pK_a$  the pores are open and influx is increased.

In another contribution, Li *et al.* grafted pNIPAM *via* ATRP in the pores of AAO membranes.<sup>95</sup> They analyze the gating functionality of the membrane by the permeation of vitamin B12. They observe a strong increase of permeability by heating above the LCST of pNIPAM, due to the collapse of the blocking polymer layer. This system thus displayed a positive gating effect. Moreover, the thermo-responsive switching of the gates was preserved for three consecutive closed-opened cycles. Very recently, Lee *et al.*<sup>96</sup> reported for a similarly prepared



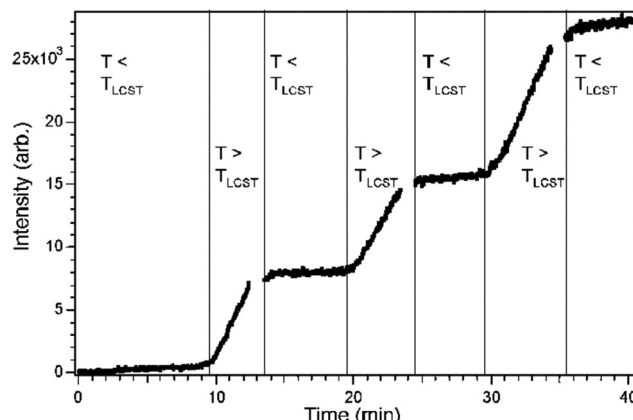


Fig. 9 Reversible switching capability of the pNIPAM grafted membrane. Permeation of 77 kDa dextran over several heating–cooling cycles measured over time *via* fluorescence. At each gate opening, the dextran concentration increases resulting in a higher intensity. Reprinted with permission from Lokuge, I. *et al.* (2007), **23**(1), 305–311. Copyright 2007 American Chemical Society.

AAO-g-pNIPAM membrane a decrease in resistance with increasing temperature due to the positive gating effect.

As already mentioned, Lokuge *et al.*<sup>81</sup> grafted pNIPAM brushes on a gold-coated nanocapillary array membrane (NCAM) *via* ATRP to control the thickness of the pNIPAM brushes. They investigated the flow of dextran of different molecular weight through different pore size NCAMs with different pNIPAM brush thicknesses. Below the NIPAM LCST the dextran flow through the NCAM was inhibited due to brush swelling, while above the LCST dextran could flow through the NCAM. This behavior evidences a positive gating effect. These authors were thus able to produce a thermoresponsive molecular gate. Fig. 9 shows the dextran concentration on one side of the membrane measured by UV-spectroscopy, while the other side is a dextran reservoir. Each time the temperature is above the LCST, the gates open and the dextran concentration increases further, while it stays constant when the gates are closed below the LCST.

## V. Conclusion

In the field of gating membranes, several extended review articles or entire book chapters dedicated to this subject exist, see for instance<sup>24</sup> and.<sup>97</sup> In the present short contribution, we have highlighted about 35 very recent articles, as well as some precursor work, reporting the formation, properties, and applications of smart membranes based on either “all-smart” or functionalized porous membranes. Because of their widespread use, we have focused the review on the temperature effect and on the use of microgels as functional component of the membranes. We termed “positive gating” the property of the system to increase flux (of solvents, particles, contaminants...) with increasing temperature, and “negative gating” the opposite behavior, and tried to identify where possible in which category each example fell. We have also included works which may possibly be useful for the formation of smart membranes,

like novel support membranes, even if to our best knowledge they have not yet been used to produce smart gating membranes.

Most of the effects have been characterized by permeation experiments. In some cases, microscopic observation allowed evidencing pore opening or closing. Given the fundamental question of how the pores are really closed, we think it would be of interest to go further towards microscopic characterization, which in the field of polymer physics is often performed by scattering techniques. Indeed, grazing-incidence, reflectometry, or small-angle scattering of neutrons or X-rays would give access to polymer conformations as a function of the external stimulus, which could then be correlated with permeation experiments. We have found only limited use of these techniques in the literature, and it is hoped to see more applications of these techniques in the future.

One of the key questions which arises when reviewing the most recent contributions is if it is “better” to use temperature-sensitive individual polymer chains (*e.g.* as smart pore coating), or deposit larger microgel particles and possibly crosslink them together (“all smart”). While the discussion is still open, we note that microgel particles have the advantage of being visible *via* microscopy at the single-building block scale of the membrane. Moreover, their degree of smartness can be tuned by internal crosslinking. One can imagine, *e.g.*, that tuning the ratio between primary and secondary crosslinking “tightens” the network between two limiting cases, the one of strong particles loosely connected, and the inverse, a strong percolating network filled with fuzzy particles, each case having a different temperature response due to the different degrees of hydrophobicity of each crosslinker. Also, their larger and controllable size can be used to design both “pore covering” and “pore filling” mechanisms. Last but not least, their larger size can be used to prepare membranes with larger pores, and thus higher throughput when the gates are open, while retention is already high with a single microgel layer. On the other hand, da Silva showed that one can get good variation of the flux (and low flux) by grafting individual pNIPAM chains on 5-micron pores, which is highly promising.<sup>80</sup>

It appears that although continuous progress has been made in the field over the past years, future work should couple fundamental understanding with improved gating properties. This may include better permeation when pores are open, allowing for higher fluxes, while efficiently blocking flux when closed. One can also imagine adding functions to the gating membranes, like embedded catalytic particles (see Sabadasch *et al.*<sup>55</sup>) which could favor a desired reaction, like decomposition of some pollutant during filtering. Given the many possible applications, in particular those related to environmental issues (decontamination, waste-water treatment, controlled catalytic reactions...), we are looking forward to following new adventures in this field.

## Author contributions

Conceptualization: JO, DT, TH; funding acquisition: JO, TH; supervision: JO, DT, TH; writing – original draft: all authors; writing – review & editing: all authors.



## Conflicts of interest

There are no conflicts to declare.

## Acknowledgements

The authors are grateful for funding of the joint 'SmartBrane' project to the DFG (grant number 505656154) and the ANR (grant number ANR-22-CE92-0052-01).

## Notes and references

- 1 S.-C. Low and Q.-H. Ng, Progress of stimuli responsive membranes in water treatment, in *Advanced Nanomaterials for Membrane Synthesis and its Applications*, ed. W. Jye Lau, A. Fauzi Ismail, A. M. Isloor and A. Al-Ahmed, Elsevier, 2019. pp. 69–99.
- 2 T. Huang, Z. Su, K. Hou, J. Zeng, H. Zhou, L. Zhang and S. P. Nunes, *Chem. Soc. Rev.*, 2023, **52**(13), 4173.
- 3 A. Darabi, P. G. Jessop and M. F. Cunningham, *Chem. Soc. Rev.*, 2016, **45**(15), 4391.
- 4 S. Kumar, X. Tong, Y. L. Dory, M. Lepage and Y. Zhao, *Chem. Commun.*, 2013, **49**(1), 90.
- 5 H. Che, M. Huo, L. Peng, T. Fang, N. Liu, L. Feng, Y. Wei and J. Yuan, *Angew. Chem., Int. Ed.*, 2015, **54**(31), 8934.
- 6 Y. Qiu and K. Park, *Adv. Drug Delivery Rev.*, 2001, **53**(3), 321.
- 7 T. Aoki, M. Muramatsu, T. Torii, K. Sanui and N. Ogata, *Macromolecules*, 2001, **34**(10), 3118.
- 8 H. Alem, A.-S. Duwez, P. Lussis, P. Lipnik, A. M. Jonas and S. Demoustier-Champagne, *J. Membr. Sci.*, 2008, **308**(1–2), 75.
- 9 M. Cors, O. Wrede, A.-C. Genix, D. Anselmetti, J. Oberdisse and T. Hellweg, *Langmuir*, 2017, **33**(27), 6804.
- 10 M. Cors, L. Wiehemeier, J. Oberdisse and T. Hellweg, *Polymers*, 2019, **11**(4), 620.
- 11 F. Schneider, A. Balaceanu, A. Feoktystov, V. Pipich, Y. Wu, J. Allgaier, W. Pyckhout-Hintzen, A. Pich and G. J. Schneider, *Langmuir*, 2014, **30**(50), 15317.
- 12 F. Scheffold, *Nat. Commun.*, 2020, **11**(1), 4315.
- 13 J. Es Sayed, M. Khoonkari, M. Oggioni, P. Perrin, N. Sanson, M. Kamperman and M. K. Włodarczyk-Biegum, *Adv. Funct. Mater.*, 2022, **32**(48), 2207816.
- 14 J. Es Sayed, C. Lorthioir, P. Banet, P. Perrin and N. Sanson, *Angew. Chem., Int. Ed.*, 2020, **59**(18), 7042.
- 15 H. Bachman, A. C. Brown, K. C. Clarke, K. S. Dhada, A. Douglas, C. E. Hansen, E. Herman, J. S. Hyatt, P. Kodekere, Z. Meng, S. Saxena, M. W. Spears, N. Welsch and L. A. Lyon, *Soft Matter*, 2015, **11**(10), 2018.
- 16 K. Kratz, A. Lapp, W. Eimer and T. Hellweg, *Colloids Surf., A*, 2001, **197**, 55–67.
- 17 T. Sato, N. Higashida, T. Hirano and M. Seno, *J. Polym. Sci., Part A: Polym. Chem.*, 2004, **42**(7), 1609.
- 18 M. Dirksen, P. Fandrich, L. Goett-Zink, J. Cremer, D. Anselmetti and T. Hellweg, *Langmuir*, 2022, **38**(2), 638.
- 19 S. Schmidt, M. Zeiser, T. Hellweg, C. Duschl, A. Fery and H. Möhwald, *Adv. Funct. Mater.*, 2010, **20**(19), 3235.
- 20 M. Flechner, J. Schaller, M. Stahl, K. Achberger, S. Gerike, Y. Hannappel, J. Fu, M. Jaeger, T. Hellweg, C. Duschl and K. Uhlig, *Biotechnol. Bioeng.*, 2022, **119**(7), 1728.
- 21 K. Uhlig, T. Wegener, Y. Hertle, J. Bookhold, M. Jaeger, T. Hellweg, A. Fery and C. Duschl, *Polymers*, 2018, **10**(6), 656.
- 22 M. Ulbricht and H. Yang, *Chem. Mater.*, 2005, **17**(10), 2622.
- 23 J. Kim, G. Zhang, M. Shi and Z. Suo, *Science*, 2021, **374**(6564), 212.
- 24 Z. Liu, W. Wang, R. Xie, X.-J. Ju and L.-Y. Chu, *Chem. Soc. Rev.*, 2016, **45**(3), 460.
- 25 Y. Pan, Y. Liu, S. Yang, C. Zhang and Z. Ullah, *Nanotechnol. Rev.*, 2023, **12**(1), 20220538.
- 26 S. Friesen, Y. Hannappel, S. Kakorin and T. Hellweg, *Colloid Polym. Sci.*, 2022, **300**(11), 1235.
- 27 S. Y. Park and Y. H. Bae, *Macromol. Rapid Commun.*, 1999, **20**(5), 269.
- 28 V. H. Pino-Ramos, A. Ramos-Ballesteros, F. López-Saucedo, J. E. López-Barriguete, G. H. C. Varca and E. Bucio, Radiation Grafting for the Functionalization and Development of Smart Polymeric Materials, in *Applications of Radiation Chemistry in the Fields of Industry, Biotechnology and Environment. Topics in Current Chemistry Collections*, ed. M. Venturi and M. D'Angelantonio, Springer International Publishing, Cham, 2017. pp.67–94.
- 29 N. A. Patil and B. Kandasubramanian, *Eur. Polym. J.*, 2021, **146**, 110248.
- 30 Y. M. Mohan and K. E. Geckeler, *React. Funct. Polym.*, 2007, **67**(2), 144.
- 31 A. Singh, S. S. Narvi, P. K. Dutta and N. D. Pandey, *Bull. Mater. Sci.*, 2006, **29**(3), 233.
- 32 A. Pich and W. Richtering, Microgels by Precipitation Polymerization: Synthesis, Characterization, and Functionalization, in *Chemical Design of Responsive Microgels. Advances in Polymer Science*, ed. A. Pich and W. Richtering, Springer Berlin Heidelberg, Berlin, Heidelberg, 2011. pp.1–37.
- 33 N. P. Truong, G. R. Jones, K. G. E. Bradford, D. Konkolewicz and A. Anastasaki, *Nat. Rev. Chem.*, 2021, **5**(12), 859.
- 34 M. Karg, A. Pich, T. Hellweg, T. Hoare, L. A. Lyon, J. J. Crassous, D. Suzuki, R. A. Gumerov, S. Schneider, I. I. Potemkin and W. Richtering, *Langmuir*, 2019, **35**(19), 6231.
- 35 *Advanced Nanomaterials for Membrane Synthesis and its Applications*, ed. W. Jye Lau, A. Fauzi Ismail, A. M. Isloor and A. Al-Ahmed, Elsevier, 2019.
- 36 G. L. Li, H. Möhwald and D. G. Shchukin, *Chem. Soc. Rev.*, 2013, **42**(8), 3628.
- 37 M. Kato, M. Kamigaito, M. Sawamoto and T. Higashimura, *Macromolecules*, 1995, **28**(5), 1721.
- 38 J.-S. Wang and K. Matyjaszewski, *J. Am. Chem. Soc.*, 1995, **117**(20), 5614.
- 39 E. A. Appel, J. Del Barrio, X. J. Loh and O. A. Scherman, *Chem. Soc. Rev.*, 2012, **41**(18), 6195.
- 40 M. Shibayama, T. Tanaka and C. C. Han, *J. Chem. Phys.*, 1992, **97**(9), 6842.
- 41 F. Horkay, A. M. Hecht, S. Mallam, E. Geissler and A. R. Rennie, *Macromolecules*, 1991, **24**(10), 2896.



42 M. Dirksen, T. Brändel, S. Großkopf, S. Knust, J. Bookhold, D. Anselmetti and T. Hellweg, *RSC Adv.*, 2021, **11**(36), 22014.

43 D. J. Bell, S. Ludwanowski, A. Lüken, B. Sarikaya, A. Walther and M. Wessling, *J. Membr. Sci.*, 2021, **620**, 118912.

44 T. Still, P. J. Yunker, K. Hanson, Z. S. Davidson, M. A. Lohr, K. B. Aptowicz and A. G. Yodh, *Adv. Mater. Interfaces*, 2015, **2**(16), 1500371.

45 T. Kajornprai, P. Katesripongsa, S. Y. Nam, Z. A. A. Hamid, Y. Ruksakulpiwat, N. Suppakarn and T. Trongsatitkul, *Polymers*, 2023, **15**(3), 497.

46 M. S. Kim, S. J. Lee, J. U. Kang and K. J. Bae, *J. Ind. Eng. Chem.*, 2005, **11**(2), 187.

47 H. Cong, X. Xu, B. Yu, Z. Yang and X. Zhang, *Sci. Rep.*, 2016, **6**, 32130.

48 A. L. Medina-Castillo, L. Ruzic, B. Nidetzky and J. M. Bolivar, *ACS Appl. Polym. Mater.*, 2022, **4**(8), 6054.

49 O. Nir, T. Trieu, S. Bannwarth and M. Wessling, *Soft Matter*, 2016, **12**(31), 6512.

50 G. Vitola, D. Büning, J. Schumacher, R. Mazzei, L. Giorno and M. Ulbricht, *Macromol. Biosci.*, 2017, **17**(5), 1600381.

51 A. Wirsén and A.-C. Albertsson, *J. Polym. Sci., Part A: Polym. Chem.*, 1995, **33**(12), 2039.

52 J. Bookhold, M. Dirksen, L. Wiehemeier, S. Knust, D. Anselmetti, F. Paneff, X. Zhang, A. Gölzhäuser, T. Kottke and T. Hellweg, *Soft Matter*, 2021, **17**(8), 2205.

53 S. Jauk and R. Liska, *Macromol. Rapid Commun.*, 2005, **26**(21), 1687.

54 J. Zhou, X. Allonas, A. Ibrahim and X. Liu, *Prog. Polym. Sci.*, 2019, **99**, 101165.

55 V. Sabadasch, M. Dirksen, P. Fandrich, J. Cremer, N. Biere, D. Anselmetti and T. Hellweg, *ACS Appl. Mater. Interfaces*, 2022, **14**(43), 49181.

56 J. Kawahara, K. Ishikawa, T. Uchimaru and H. Takaya, Chemical Cross-Linking by Glutaraldehyde between Amino Groups: Its Mechanism and Effects, in *Polymer Modification*, ed. G. Swift, C. E. Carraher and C. N. Bowman, Springer, Boston, MA, 1997. pp.119–31.

57 I. Tokarev, V. Gopishetty and S. Minko, *ACS Appl. Mater. Interfaces*, 2015, **7**(23), 12463.

58 F. Peng, Z. Jiang, C. Hu, Y. Wang, H. Xu and J. Liu, *Sep. Purif. Technol.*, 2006, **48**(3), 229.

59 F. Ahmed, A. Hategan, D. E. Discher and B. M. Discher, *Langmuir*, 2003, **19**(16), 6505.

60 A. El Haitami, E. H. G. Backus and S. Cantin, *Langmuir*, 2014, **30**(40), 11919.

61 S. Coppola, L. Miccio, Z. Wang, G. Nasti, V. Ferraro, P. L. Maffettone, V. Vespi, R. Castaldo, G. Gentile and P. Ferraro, *RSC Adv.*, 2022, **12**(48), 31215.

62 M. Cetintas, J. de Groot, A. H. Hofman, H. M. van der Kooij, K. Loos, W. M. de Vos and M. Kamperman, *Polym. Chem.*, 2017, **8**(14), 2235.

63 J. D. Willott, W. M. Nielen and W. M. de Vos, *ACS Appl. Polym. Mater.*, 2020, **2**(2), 659.

64 S. Schmidt, H. Motschmann, T. Hellweg and R. von Klitzing, *Polymer*, 2008, **49**(3), 749.

65 V. Nigro, E. Buratti, F. Limosani, R. Angelini, F. Dinelli, S. Franco, E. Nichelatti, M. Piccinini, M. A. Vincenti, R. M. Montereali and B. Ruzicka, *Colloids Surf., A*, 2023, **674**, 131918.

66 M. F. Schulte, A. Scotti, M. Brugnoni, S. Bochenek, A. Mourran and W. Richtering, *Langmuir*, 2019, **35**(46), 14769.

67 E. Kang, J. Ryoo, G. S. Jeong, Y. Y. Choi, S. M. Jeong, J. Ju, S. Chung, S. Takayama and S.-H. Lee, *Adv. Mater.*, 2013, **25**(15), 2167.

68 A. L. Thangawng, R. S. Ruoff, M. A. Swartz and M. R. Glucksberg, *Biomed. Microdevices*, 2007, **9**(4), 587.

69 A. Nykänen, M. Nuopponen, A. Laukkanen, S.-P. Hirvonen, M. Rytelä, O. Turunen, H. Tenhu, R. Mezzenga, O. Ikkala and J. Ruokolainen, *Macromolecules*, 2007, **40**(16), 5827.

70 Y. Tang, K. Ito, L. Hong, T. Ishizone and H. Yokoyama, *Macromolecules*, 2016, **49**(20), 7886.

71 C. Cutright, Z. Brotherton, L. Alexander, J. Harris, K. Shi, S. Khan, J. Genzer and S. Menegatti, *Appl. Surf. Sci.*, 2020, **508**, 145129.

72 Y. Xia, X. He, M. Cao, C. Chen, H. Xu, F. Pan and J. R. Lu, *Biomacromolecules*, 2013, **14**(10), 3615.

73 T. Lohaus, P. de Wit, M. Kather, D. Menne, N. E. Benes, A. Pich and M. Wessling, *J. Membr. Sci.*, 2017, **539**, 451.

74 Y. Xu, A. Ajji and M.-C. Heuzey, *Polymer*, 2019, **183**, 121880.

75 S. Zhang, Q. Su, J. Yan, Z. Wu, L. Tang, W. Xiao, L. Wang, X. Huang and J. Gao, *Chem. Eng. Sci.*, 2022, **264**, 118175.

76 T. V. Plisko, A. V. Bildyukevich, K. S. Burts, T. A. Hliavitskaya, A. V. Penkova, S. S. Ermakov and M. Ulbricht, *Membranes*, 2020, **10**(10), 264.

77 W. Wei, W. Zhang, Q. Jiang, P. Xu, Z. Zhong, F. Zhang and W. Xing, *J. Membr. Sci.*, 2017, **540**, 381.

78 L. Chen, K. Guan, W. Zhu, C. Peng and J. Wu, *RSC Adv.*, 2018, **8**(70), 39884.

79 F. Chen, X. Jiang, T. Kuang, L. Chang, D. Fu, Z. Yang, J. Yang, P. Fan, Z. Fei and M. Zhong, *RSC Adv.*, 2015, **5**(86), 70204.

80 M. J. Da Enes Silva, A. Banerjee, L. Lefferts and J. A. Faria Albanese, *ChemCatChem*, 2022, **14**(10), e202101835.

81 I. Lokuge, X. Wang and P. W. Bohn, *Langmuir*, 2007, **23**(1), 305.

82 H. Böttcher, M. L. Hallensleben, S. Nuß, H. Wurm, J. Bauer and P. Behrens, *J. Mater. Chem.*, 2002, **12**(5), 1351.

83 A. Friebel and M. Ulbricht, *Langmuir*, 2007, **23**(20), 10316.

84 L. Ionov, N. Houbenov, A. Sidorenko, M. Stamm and S. Minko, *Adv. Funct. Mater.*, 2006, **16**(9), 1153.

85 B. P. Tripathi, N. C. Dubey and M. Stamm, *ACS Appl. Mater. Interfaces*, 2014, **6**(20), 17702.

86 S. Maity, D. Gaur, B. Mishra, N. C. Dubey and B. P. Tripathi, *J. Colloid Interface Sci.*, 2023, **642**, 129.

87 S. Maity, B. Mishra, K. Nayak, N. C. Dubey and B. P. Tripathi, *Mater. Today Chem.*, 2022, **24**, 100779.

88 B. Mishra, S. Biswal, N. C. Dubey and B. P. Tripathi, *ACS Appl. Polym. Mater.*, 2022, **4**(7), 4719.

89 N. H. Othman, N. H. Alias, N. S. Fuzil, F. Marpani, M. Z. Shahruddin, C. M. Chew, K. M. David Ng, W. J. Lau and A. F. Ismail, *Membranes*, 2021, **12**(1), 30.

90 U. Hani, *Alexandria Eng. J.*, 2023, **72**, 307.



91 O. Wrede, Y. Reimann, S. Lülsdorf, D. Emmrich, K. Schneider, A. J. Schmid, D. Zauser, Y. Hannappel, A. Beyer, R. Schweins, A. Gölzhäuser, T. Hellweg and T. Sottmann, *Sci. Rep.*, 2018, **8**(1), 13781.

92 D. Menne, F. Pitsch, J. E. Wong, A. Pich and M. Wessling, *Angew. Chem., Int. Ed.*, 2014, **53**(22), 5706.

93 M. Wiese, T. Lohaus, J. Haussmann and M. Wessling, *J. Membr. Sci.*, 2019, **588**, 117190.

94 Y. Ding, G. Panzarasa, S. Stucki, I. Burgert and T. Keplinger, *ACS Sustainable Chem. Eng.*, 2022, **10**(17), 5517.

95 P.-F. Li, R. Xie, J.-C. Jiang, T. Meng, M. Yang, X.-J. Ju, L. Yang and L.-Y. Chu, *J. Membr. Sci.*, 2009, **337**(1–2), 310.

96 M.-J. Lee, Y.-F. Chen, L.-R. Lee, Y.-L. Lin, S. Zheng, M.-H. Chang and J.-T. Chen, *Chemistry*, 2023, **29**(43), e202301012.

97 R. Ghosh, Stimuli-Responsive Membranes for Separations, in *Functional Biopolymers. Polymers and Polymeric Composites: A Reference Series*, ed. M. A. Jafar Mazumder, H. Sheardown and A. Al-Ahmed, Springer International Publishing, Cham, 2019, pp.491–508.

